Archive of Applied Mechanics 69 (1999) 751–764 © Springer-Verlag 1999

Shakedown analysis of defective pressure vessels by a kinematic approach

V. Carvelli, Z. Z. Cen, Y. Liu, G. Maier

Summary In this paper, a kinematic approach and an iterative procedure, earlier proposed for limit analysis, are adopted for shakedown analysis under variable repeated loading. Reference is made to three-dimensional structures of engineering relevance, such as pressurized pipelines and vessels with fluctuating pressure and with slot damages due, e.g. to pitting corrosion. The numerical performance of the solution algorithm is investigated, and the cost-effectiveness of the proposed direct shakedown analysis method is assessed and compared to that of time-marching solutions by up-to-date codes.

Key words plasticity, shakedown, kinematic approach, pressure vessels, initial defect

1 Introduction

Ductile structures subjected to variable repeated (in particular, cyclic) external actions are exposed to structural failures which mature as time elapses, either by incremental collapse (or ratchetting) or by alternating plasticity (or low cycle fatigue). The contrary events, named shakedown or "adaptation" in the plasticity literature (as probably proposed by William Prager), is characterized by the circumstance that plastic yielding eventually ceases, namely by bounded cumulative energy dissipation. The abundant literature on shakedown theory, analysis and design, pioneered by Melan in this Journal, [21], will not be surveyed herein; fairly comprehensive critical reviews can be found, e.g. in [14] and in treatises on plasticity such as [8, 18]. While Melan's static approach gave rise to many developments in computational mechanics, numerical solutions based on Koiter's kinematic theorem [12, 15] are still rare. The main reasons lie in the difficulty of handling admissible plastic strain cycles and the time dependence embodied in Koiter's original statement. In previous kinematic shakedown analyses, linear programming techniques were developed by using piece-wise linear (Tresca) or linearized yield criterion, e.g. [11, 23]. The application of von Mises criterion leads to a nonlinear mathematical programming problem, the solution of which in practical engineering applications with complex structures and loading still represents a challenge.

The contents and purposes of this paper are as follows: the shakedown (henceforth SD) analysis is formulated in Sec. 2 for 3d continua by a kinematic approach based on classical concepts and theorems due to Symonds and Neal [24] and Koiter [12]. Linear kinematics ("small deformations") and Drucker's stability of materials are assumed as basic hypotheses von Mises elastoplastic model is adopted as a specialization in view of the ductile metal structures considered in the examples; the removal of time is performed, leading to an unconstrained minimization in convex "nonsmooth" mathematics. The finite element space-discretization, described in Sec. 3, leads to a mathematical programming problem

Received 28 May 1999; accepted for publication 8 June 1999

V. Carvelli, G. Maier
Department of Structural Engineering,
Technical University (Politecnico) of Milan,
Piazza Leonardo Da Vinci 32, I-20133 Milan, Italy

Z. Z. Cen, Y. Liu
Department of Engineering Mechanics, Tsinghua University,
Beijing 100084, P. R. China

This paper is dedicated to the memory of Professor
P. D. Panagiotopoulos.

characterized by nonsmoothness of the objective function and by equality constraints. The iterative solution algorithm proposed for limit analysis in [25] is expounded in Sec. 4 with adjustments dictated by earlier, [16], and present peculiarities of the tackled problems. The computational tests outlined in Sec. 5 lead to an understanding of potentialities and limitations of the main provisions of the algorithm adopted, namely penalization, Lagrange multipliers, user-available tolerances. Evolutive step-by-step analyses of the same situations permit a rather meaningful comparative assessment of computational merits of the proposed direct ("simplified") method, which turns out to be significantly advantageous in many real-life engineering situations. In general, it should be kept in mind that time-marching solutions may be not only expensive (and even prohibitive for parametric studies in design processes), but also unreliable when the loading history cannot be a-priori predicted with any accuracy. Concluding remarks are gathered in the last Section.

2
Problem formulation by a kinematic approach

2.1
Assumptions

The considered solid occupies the volume V with boundary surface S and is subjected to tractions p_i on part S_t of the boundary surface (assumed for brevity as the only external actions) and prescribed displacements on the remaining part $S_u = S - S_t$ (i runs over the axes of a cartesian reference frame x_1, x_2, x_3).

The following hypotheses are assumed: displacement gradients are regarded as "small", so that the kinematic relations are linear; the loads vary slowly in time (i.e. give rise to a quasi-static structural response); the material is elastic-perfectly plastic and stable in Drucker's sense.

The last hypothesis concerning the constitutive models materializes in the following customary relationships, [8, 18]:

$$\varepsilon_{ij} = \varepsilon^e_{ij} + \varepsilon^p_{ij}, \quad \varepsilon^e_{ij} = C_{ijkh}\sigma_{kh} \ , \tag{1}$$

$$\phi(\sigma_{ij}) \leq 0 \ , \tag{2}$$

$$\dot{\varepsilon}^p_{ij} = \dot{\lambda}\frac{\partial\phi}{\partial\sigma_{ij}}, \quad \dot{\lambda} \geq 0, \quad \phi\dot{\lambda} = 0 \ . \tag{3}$$

Equation (1a) expresses the assumed additive decomposition of the strain tensor ε_{ij} $(i, j, k, h = 1, 2, 3)$; the elastic addend ε^e_{ij} is linearly related to the stress tensor σ_{ij} through the elastic compliance tensor C_{ijkh} endowed with the usual symmetries. The convex yield function ϕ defines the material strength by inequality (2); it is involved in the "normality rule", Eq. (3a), of plastic strains $\dot{\varepsilon}^p_{ij}$ through its gradient and in "Prager consistency" of plastic flow in Eq. (3) through its complementarity relation with the plastic multiplier rate $\dot{\lambda}$.

A single yield mode is considered herein (ϕ is "smooth": no "corners"), a restriction easily removed whenever necessary.

Plastic work rate or dissipation per unit volume reads

$$D\big(\dot{\varepsilon}^p_{ij}\big) = \sigma_{ij}\dot{\varepsilon}^p_{ij} \ . \tag{4}$$

Drucker's postulate of material stability (with consequences of primary importance here, and generally, in the plasticity theory) is expressed by the inequality

$$\big(\sigma_{ij} - \sigma^*_{ij}\big)\dot{\varepsilon}^p_{ij} \geq 0 \qquad \forall\, \sigma^*_{ij} : \phi\big(\sigma^*_{ij}\big) \leq 0 \ ,$$

where σ_{ij} is the stress on the yield surface in the presence of the plastic strain rate $\dot{\varepsilon}^p_{ij}$ and σ^*_{ij} is any stress state not outside the elastic domain. As a consequence, in any infinitesimal inelastic process

$$\dot{\sigma}_{ij}\dot{\varepsilon}^p_{ij} \geq 0 \ .$$

Henceforth, von Mises' criterion will be adopted. Then, denoting by σ_0 the yield stress in uniaxial tests and by J_2 the second stress invariant, the yield function reads

$$\phi(\sigma_{ij}) = \sqrt{J_2} - \sigma_0/\sqrt{3} \ . \tag{5}$$

In view of associative flow rule (3a) and von Mises' yield function (5), the plastic dissipation (4) is expressed by, [8, 18]

$$D(\dot{\varepsilon}^p_{ij}) = \sqrt{\tfrac{2}{3}}\sigma_0 \sqrt{\dot{\varepsilon}^p_{ij}\dot{\varepsilon}^p_{ij}} \ . \tag{6}$$

2.2
Shakedown analysis concepts

Whenever a ductile structure is designed to sustain variable repeated loads (possibly beyond the elastic range in exceptionally severe conditions), structural safety requires to ensure that stabilization of plastic deformations, i.e. SD, will eventually occur. In the absence of SD, the structural response may imply either incremental collapse or alternating plasticity, having in common the circumstance that the dissipated energy cumulative in space appears to grow unboundedly in time.

Incremental collapse means that plastic deformations accumulate along the load history so that displacements become large enough to make the structure unserviceable. Alternating plasticity is characterized by the fact that the configuration changes remain small, but locally dissipative plastic processes do not stop leading to material failure.

In many engineering situations step-by-step evolutive elastic-plastic analysis turns out to be inadequate, primarily because detailed information on the load histories is not available, so that the number of loading paths to be accounted for often becomes prohibitively high.

Nonevolutive "direct" methods that consider once for all the whole set of load variations represent, in principle, a valuable and potentially cost-effective alternative. Such methods are based on the static and kinematic SD theorems, see e.g. [14, 15, 20].

By definition, "load domain" Ω represents a region in the space of the variables which govern the loading history: this time history being not a-priori predictable, any point belonging to Ω is assumed to represent a combination of external actions, which can be attained again and again, an unbounded number of times at unknown instants according to an unknown sequence. External actions will be tractions on S_t only; whenever necessary, body forces, imposed displacements on S_u and imposed (such as thermal) strains in V can be easily allowed for.

Let all possible load combinations be multiplied by a common amplification factor μ (load factor), namely: let the region Ω in the space of load variables be affected by an homotetic transformation, with the reference frame origin acting as pole. The central objective of the SD theory is to compute the "safety factor" s, i.e. the value of the load domain amplification factor μ such that for $\mu < s$ the structure does not collapse due to incremental collapse or alternating plasticity. It does, if $\mu > s$.

2.3
Kinematic shakedown theory: fundamentals

In any elastic-plastic body subjected to external actions in a "small" deformation regime, the stress field can always be conceived as the sum of two addends: $\sigma_{ij} = \sigma^e_{ij} + \rho_{ij}$, where σ^e_{ij} denotes the elastic stress response to the given external actions in a fictitious hypothetical purely elastic structural response and ρ_{ij} is the field of residual stresses, i.e. the (unique) elastic response to plastic strains, satisfying self-equilibrium equations and homogeneous static boundary conditions. Accordingly, the actual displacement field u_i can be split into two addends: $u_i = u^e_i + u^r_i$, u^r_i being residual displacements.

Koiter's kinematic SD theorem [12, 15, 18] is based on the concept of admissible plastic strain rate cycle, say $\dot{\varepsilon}^p_{ij}(x_i, t)$, defined as follows:

$$\Delta\tilde{\varepsilon}^p_{ij}(x_i) = \int_0^T \dot{\varepsilon}^p_{ij}(x_i, t)\mathrm{d}t; \quad \Delta\tilde{\varepsilon}^p_{ij} = \tfrac{1}{2}(\Delta\tilde{u}^r_{i,j} + \Delta\tilde{u}^r_{j,i}) \ . \tag{7}$$

Equation (7b) expresses geometric compatibility of the cumulative plastic strains at the end of the cycle over the time interval [0, T], denoting by $\Delta\tilde{u}^r_i$ the cumulative residual displacement field at time T due to $\dot{\varepsilon}^p_{ij}$ with homogeneous kinematic boundary conditions on S_u at any t in [0, T]. Using this definition, Koiter's theorem can be stated as follows:

A structure subjected to a given load domain Ω amplified by μ will not shake down if there exists an admissible plastic strain rate cycle $\dot{\tilde{\varepsilon}}^p_{ij}$ and a load history within Ω, such that over a time interval $[0, T]$

$$\mu \int_0^T \int_{S_t} p_i \dot{\tilde{u}}_i^r \, \mathrm{d}S \, \mathrm{d}t > \int_0^T \int_V D\left(\dot{\tilde{\varepsilon}}^p_{ij}\right) \mathrm{d}V \, \mathrm{d}t \quad . \tag{8}$$

The structure will shake down within the load domain Ω amplified by load factor μ, if for all loading paths within Ω and for all admissible plastic strain rate cycles $\dot{\tilde{\varepsilon}}^p_{ij}$, the following inequality holds:

$$\mu \int_0^T \int_{S_t} p_i \dot{\tilde{u}}_i^r \, \mathrm{d}S \, \mathrm{d}t < \int_0^T \int_V D\left(\dot{\tilde{\varepsilon}}^p_{ij}\right) \mathrm{d}V \, \mathrm{d}t \quad . \tag{9}$$

The principle of virtual work applied to the left-hand side of Eq. (8) and (9) provides

$$\int_0^T \int_{S_t} p_i \dot{\tilde{u}}_i^r \, \mathrm{d}S \, \mathrm{d}t = \int_0^T \int_V \sigma^e_{ij} \left(\dot{\tilde{\varepsilon}}^p_{ij} + C_{ijkh} \dot{\tilde{\rho}}_{kh}\right) \mathrm{d}V \, \mathrm{d}t = \int_0^T \int_V \sigma^e_{ij} \dot{\tilde{\varepsilon}}^p_{ij} \, \mathrm{d}V \, \mathrm{d}t \quad . \tag{10}$$

Here, σ^e_{ij} denotes the linear elastic stress response to the current external actions (p_i), and $\dot{\tilde{\rho}}_{ij}$ is the residual stress rate response to the admissible plastic strain rate cycle $\dot{\tilde{\varepsilon}}^p_{ij}$, interpreted as imposed in a linear elastic regime. Since $C_{ijkh}\sigma^e_{kh}$ represents a compatible strain field and $\dot{\tilde{\rho}}_{ij}$ is self-equilibrated, the relevant integral in Eqs. (10) vanishes.

By means of Eqs. (10) and by other considerations herein omitted (also on stability of the system with respect to infinitesimal perturbation), the above Koiter's statements can be reformulated in the following unified fashion:

The SD limit amplification factor s is the minimum of the following optimization problem:

$$s = \min \mu \left\{ \begin{array}{l} \mu = \int_0^T \int_V D(\dot{\tilde{\varepsilon}}^p_{ij}) \mathrm{d}V \, \mathrm{d}t, \ \text{for all admissible plastic strain rate cycles } \dot{\tilde{\varepsilon}}^p_{ij} \\ \qquad\qquad\qquad\qquad\qquad\qquad \text{such that } \int_0^T \int_V \sigma^e_{ij} \dot{\tilde{\varepsilon}}^p_{ij} \, \mathrm{d}V \, \mathrm{d}t = 1 \end{array} \right\} . \tag{11}$$

On the basis of the above definition of the admissible plastic strain rate cycle and of the present assumption of Mises yield criterion, Eqs. (5, 6) throughout the volume V, adopting matrix notation (bold-face symbols for matrices and vectors; engineering definition of strains; tilde dropped for brevity), the minimization (11) can be given the following expression:

$$s = \min_{\dot{\boldsymbol{\varepsilon}}^p, \Delta \mathbf{u}} \sqrt{\tfrac{2}{3}} \sigma_0 \int_0^T \int_V \sqrt{\dot{\boldsymbol{\varepsilon}}^{pT} \mathbf{X} \dot{\boldsymbol{\varepsilon}}^p} \, \mathrm{d}V \, \mathrm{d}t \quad , \tag{12a}$$

subject to:

$$\int_0^T \int_V \boldsymbol{\sigma}^{eT} \dot{\boldsymbol{\varepsilon}}^p \, \mathrm{d}V \, \mathrm{d}t = 1 \quad , \tag{12b}$$

$$\mathbf{Y}^T \dot{\boldsymbol{\varepsilon}}^p = 0 \quad \text{in } V, \ \forall \, t \quad , \tag{12c}$$

$$\Delta \boldsymbol{\varepsilon}^p = \int_0^T \dot{\boldsymbol{\varepsilon}}^p \, \mathrm{d}t = \mathscr{R}(\Delta \mathbf{u}) \quad \text{in } V \quad , \tag{12d}$$

$$\Delta \mathbf{u} = \mathbf{0} \quad \text{on } S_u \quad , \tag{12e}$$

where $\mathscr{R}$ is the (linear) compatibility differential operator and Eq. (12c) expresses plastic incompressibility implied by von Mises' model. In Eq. (12) it has been set:
$\mathbf{Y}^T = \{ 1 \quad 1 \quad 1 \quad 0 \quad 0 \quad 0 \}$ and $\mathbf{X} = \mathrm{diag}[\mathbf{I}, \tfrac{1}{2}\mathbf{I}]$, $\mathbf{I}$ being the identity matrix of order three.

3
Discretizations

3.1
Removal of time

The presence of time integrals in the direct formalization of Koiter theorem (see the preceding section) turns out to be computationally troublesome. With piecewise linearization of the yield criterion, by means of the concept of envelope of linear elastic response, it was proved in [19] that Koiter's kinematic approach is amenable to a minimization problem which does not involve time as variable.

With nonlinear yield criteria, a computationally convenient removal of time has been shown in [13] to be achievable under the weak assumption that the loading domain Ω consists of all loading conditions resulting from a convex linear combination of v assigned load distributions

$$\mathbf{p}(\mathbf{x}) = \sum_{k=1}^{v} \theta_k \mathbf{p}_k(\mathbf{x}), \quad \text{such that: } \sum_{k=1}^{v} \theta_k \leq 1, \quad \theta_k \geq 0, \quad k = 1, \ldots, v \ . \tag{13}$$

In other terms, Ω can be interpreted in the functional load space as a hyper polyhedron defined by points $\mathbf{p}_1, \ldots, \mathbf{p}_v$ which, therefore, will be referred to as vertices and by $\mathbf{p}_0 = \mathbf{0}$ (unloaded situation). On this basis it can be stated that [9, 10, 13]:

If a structure shakes down under any sequence of vertex loads within the set of vertices $\mathbf{p}_k$ $(k = 1, \ldots, v)$, then it shakes down under the whole (polyhedral) load domain Ω defined by those vertices.

The above statement allows to consider only loading processes, along which the load distribution $\mathbf{p}(\mathbf{x})$ equals successively the vertex distributions $\mathbf{p}_k(\mathbf{x})$, $k = 1, \ldots, v$, and remains constant over a time interval τ_k during which the admissible plastic strain cycle generates the plastic strain increment:

$$\boldsymbol{\varepsilon}_k^p(\mathbf{x}) = \int_{\tau_k} \dot{\boldsymbol{\varepsilon}}^p(\mathbf{x}, t)\mathrm{d}t, \quad \text{so that: } \Delta\boldsymbol{\varepsilon}^p = \sum_{k=1}^{v} \boldsymbol{\varepsilon}_k^p \ . \tag{14}$$

As a consequence of the above statement, the minimization (12) concerning the elastic-plastic continuum can be cast into the form

$$s = \min_{\boldsymbol{\varepsilon}_k^p, \Delta\mathbf{u}} \sqrt{\tfrac{2}{3}}\sigma_0 \sum_{k=1}^{v} \int_V \sqrt{\boldsymbol{\varepsilon}_k^{pT} \mathbf{X} \boldsymbol{\varepsilon}_k^p}\, \mathrm{d}V \ , \tag{15a}$$

subject to:

$$\sum_{k=1}^{v} \int_V \boldsymbol{\sigma}_k^{eT} \boldsymbol{\varepsilon}_k^p \, \mathrm{d}V = 1 \ , \tag{15b}$$

$$\mathbf{Y}^T \boldsymbol{\varepsilon}_k^p = 0 \quad \text{in } V, \quad k = 1, \ldots, v \ , \tag{15c}$$

$$\Delta\boldsymbol{\varepsilon}^p = \sum_{k=1}^{v} \boldsymbol{\varepsilon}_k^p = \mathscr{R}(\Delta\mathbf{u}) \quad \text{in } V \ , \tag{15d}$$

$$\Delta\mathbf{u} = \mathbf{0} \quad \text{on } S_u \ . \tag{15e}$$

It is worth noting that the plastic incompressibility, being a constitutive feature, is enforced at each vertex for the relevant plastic strain subincrement, Eq. (15c), while geometric compatibility is imposed on the cumulative plastic strains of the admissible cycle, Eq. (15d).

3.2
Finite element modelling

The discretization in space of problem (15) can be carried out by standard finite element procedures, say by setting over each element e

$$\Delta \mathbf{u}_e(\mathbf{x}) = \mathbf{N}_e(\mathbf{x})\Delta \mathbf{U}_e, \quad \Delta \varepsilon_e^p(\mathbf{x}) = \mathbf{B}_e(\mathbf{x})\Delta \mathbf{U}_e \ , \tag{16}$$

where $\Delta \mathbf{U}_e$ is the vector of nodal displacements, $\mathbf{N}_e$ is the shape function matrix and $\mathbf{B}_e$ the consequent compatibility matrix. Now let the assemblage of finite elements in the aggregate be performed; let the kinematic boundary conditions (here, assumed homogeneous) be enforced on constrained nodes and the integrals be approximated by Gauss formulae. Then the following algebrized version of the kinematic SD analysis (15) is achieved:

$$s = \min_{\boldsymbol{\varepsilon}_{kr}^p, \Delta \mathbf{U}} \sqrt{\tfrac{2}{3}}\sigma_0 \sum_{k=1}^{v} \sum_{r=1}^{n} W_r |\mathbf{J}|_r \sqrt{\boldsymbol{\varepsilon}_{kr}^{pT} \mathbf{X} \boldsymbol{\varepsilon}_{kr}^p} \ , \tag{17a}$$

subject to

$$\sum_{k=1}^{v} \sum_{r=1}^{n} W_r |\mathbf{J}|_r \boldsymbol{\sigma}_{kr}^{eT} \boldsymbol{\varepsilon}_{kr}^p = 1 \ , \tag{17b}$$

$$\mathbf{Y}^T \boldsymbol{\varepsilon}_{kr}^p = 0, \quad r = 1, \ldots, n, \qquad k = 1, \ldots, v \ , \tag{17c}$$

$$\Delta \boldsymbol{\varepsilon}_r^p = \sum_{k=1}^{v} \boldsymbol{\varepsilon}_{kr}^p = \mathbf{B}_r \Delta \mathbf{U}, \quad r = 1, \ldots, n \ , \tag{17d}$$

where index r runs over the set G of the n Gauss integration points ($r = 1, \ldots, n$), W and $|\mathbf{J}|$ represent the Gauss integration weight and the determinant of the Jacobian matrix of the map, respectively, vector $\Delta \mathbf{U}$ contains all unconstrained nodal displacements of the finite element model, $\mathbf{B}_r$ is the assembled compatibility matrix for strains at Gauss point r.

The above outlined discretizations with respect to time and space reduce the optimization problem (12) to an algebraic (mathematical programming) problem in finite-dimensional vector space. It might be proven, like in [19] for piecewiselinearized yield criteria, that duality theory of mathematical programming provides a meaningful link between the kinematic formulation (12) of the SD analysis and the static formulation based on Melan theorem, which was presented in this Journal in 1938, [21].

4
Solution algorithm

4.1
Unconstrained minimization and optimality conditions

As expected, problem (17) is mathematically similar to, and a generalization of, the mathematical problem arising in rigid plastic limit analysis by a kinematic approach, [16]. Its peculiar features are: linear equality constraints, objective function nondifferentiable (non-smooth) in the origin, possible "locking" phenomena due to the combination of incompressibility requirement and displacement modelling.

The algorithm proposed and successfully tested for limit analysis in [16, 17] is adopted herein and outlined below. Its basic features are: (a) plastic incompressibility, Eq. (17c), is enforced in a "soft" way by penalization, suitably choosing a single penalization factor, say α; (b) the normalization constraint, Eq. (17b), and the geometric compatibility, Eq. (17d), are dealt with by Lagrange multipliers, say λ and $\mathbf{L}_r$ (index r running over the Gauss points set G: $r \in G$).

The Lagrangian function arising from problem (17), to be tackled in accordance with (a) and (b), reads

$$\begin{aligned} \mathscr{L}(\boldsymbol{\varepsilon}_{kr}^p, \Delta \mathbf{U}, \lambda, \mathbf{L}_r) = {} & \sqrt{\tfrac{2}{3}}\sigma_0 \sum_{k=1}^{v} \sum_{r=1}^{n} W_r |\mathbf{J}|_r \sqrt{\boldsymbol{\varepsilon}_{kr}^{pT} \mathbf{X} \boldsymbol{\varepsilon}_{kr}^p} + \lambda \left(1 - \sum_{k=1}^{v} \sum_{r=1}^{n} W_r |\mathbf{J}|_r \boldsymbol{\sigma}_{kr}^{eT} \boldsymbol{\varepsilon}_{kr}^p \right) \\ & + \sum_{r=1}^{n} \mathbf{L}_r^T \left(\sum_{k=1}^{v} \boldsymbol{\varepsilon}_{kr}^p - \mathbf{B}_r \Delta \mathbf{U} \right) + \frac{1}{2} \alpha \sum_{k=1}^{v} \sum_{r=1}^{n} W_r |\mathbf{J}|_r \boldsymbol{\varepsilon}_{kr}^{pT} \mathbf{Y} \mathbf{Y}^T \boldsymbol{\varepsilon}_{kr}^p \ . \end{aligned} \tag{18}$$

The Kuhn-Tucker stationarity conditions characterizing the solution to problem (17) flow from Eq. (18) in the form

$$\frac{\partial \mathscr{L}}{\partial \varepsilon_{kr}^{p}} = \sqrt{\tfrac{2}{3}}\sigma_0 W_r |\mathbf{J}|_r \frac{\mathbf{X}\boldsymbol{\varepsilon}_{kr}^{p}}{\sqrt{\boldsymbol{\varepsilon}_{kr}^{pT}\mathbf{X}\boldsymbol{\varepsilon}_{kr}^{p}}} - \lambda W_r |\mathbf{J}|_r \boldsymbol{\sigma}_{kr}^{e} + \mathbf{L}_r + \alpha W_r |\mathbf{J}|_r \mathbf{Y}\mathbf{Y}^T \boldsymbol{\varepsilon}_{kr}^{p} = \mathbf{0},$$

$$r = 1, \ldots, n, \quad k = 1, \ldots, v \ , \tag{19a}$$

$$\frac{\partial \mathscr{L}}{\partial \Delta \mathbf{U}} = \sum_{r=1}^{n} \mathbf{B}_r^T \mathbf{L}_r = \mathbf{0} \ , \tag{19b}$$

$$\frac{\partial \mathscr{L}}{\partial \lambda} = \sum_{k=1}^{v} \sum_{r=1}^{n} W_r |\mathbf{J}|_r \boldsymbol{\sigma}_{kr}^{eT} \boldsymbol{\varepsilon}_{kr}^{p} - 1 = 0 \ , \tag{19c}$$

$$\frac{\partial \mathscr{L}}{\partial \mathbf{L}_r} = \sum_{k=1}^{v} \boldsymbol{\varepsilon}_{kr}^{p} - \mathbf{B}_r \Delta \mathbf{U} = \mathbf{0}, \quad r = 1, \ldots, n \ . \tag{19d}$$

4.2
Iterative scheme

The nonlinear equations (19) in the unknowns ε_{kr}^{p}, $\Delta\mathbf{U}$, λ, $\mathbf{L}_r$ ($r = 1, \ldots, n$, $k = 1, \ldots, v$) exhibit nonlinearity confined to the denominators in Eq. (19a) and, hence, provide linear equations at iteration h if these denominators indicated henceforth by D_{kr} are computed on the basis of results from iteration $h - 1$, namely

$$D_{kr}^{h-1} = \left(\varepsilon_{kr}^{p T^{h-1}} \mathbf{X} \varepsilon_{kr}^{p^{h-1}} \right)^{1/2} \ .$$

These remarks suggest an iterative solution procedure centered on the following equation system derived from Eqs. (19):

$$\mathbf{H}_{kr}^{h-1} \boldsymbol{\varepsilon}_{kr}^{p^h} - \lambda^h \boldsymbol{\sigma}_{kr}^{e} + (W_r |\mathbf{J}|_r)^{-1} \mathbf{L}_r^h = \mathbf{0}, \quad r = 1, \ldots, n, \quad k = 1, \ldots, v \ , \tag{20a}$$

$$\sum_{r=1}^{n} \mathbf{B}_r^T \mathbf{L}_r^h = \mathbf{0} \ , \tag{20b}$$

$$\sum_{k=1}^{v} \sum_{r=1}^{n} W_r |\mathbf{J}|_r \boldsymbol{\sigma}_{kr}^{eT} \boldsymbol{\varepsilon}_{kr}^{p^h} = 1 \ , \tag{20c}$$

$$\sum_{k=1}^{v} \boldsymbol{\varepsilon}_{kr}^{p^h} = \mathbf{B}_r \Delta \mathbf{U}^h, \quad r = 1, \ldots, n \ , \tag{20d}$$

having set

$$\mathbf{H}_{kr}^{h-1} = \sqrt{\tfrac{2}{3}}\sigma_0 \mathbf{X} \left(D_{kr}^{h-1} \right)^{-1} + \alpha \mathbf{Y}\mathbf{Y}^T \ . \tag{21}$$

Each one of denominators D_{kr}^{h-1} is proportional to the plastic dissipated energy density at Gauss point r related to the fictitious yielding process concerning load domain vertex k.

At the end of iteration $h - 1$, for each vertex k, let the set of Gauss integration points G be subdivided into a subset P_k^{h-1} ("plastic zone") of the points where dissipation occurs and the complementary subset R_k^{h-1} ("nonyielding zone") of the points where the computed plastic strains are such that the denominator D_{kr}^{h-1} is below a suitable chosen tolerance $\beta \ll 1$. Following [25], we select another available parameter $\gamma \ll 1$ and set

$$D_{kr}^{h-1} = \begin{cases} \sqrt{\boldsymbol{\varepsilon}_{kr}^{p^{T^{h-1}}} \mathbf{X} \boldsymbol{\varepsilon}_{kr}^{p^{h-1}}} & \forall\, r \in P_k^{h-1}, \\ \gamma & \forall\, r \in R_k^{h-1} \ . \end{cases} \tag{22}$$

At each iteration h, denoting by N the number of nodal degrees of freedom, the $(6nv + 1 + N + 6n)$ linear equations (20) must be solved in the unknowns $\boldsymbol{\varepsilon}_{kr}^{p^h}, \Delta\mathbf{U}^h, \lambda^h, \mathbf{L}_r^h$ $(r = 1, \ldots, n,\ k = 1, \ldots, v)$. Note that at each Gauss point r the Lagrange multiplier vector $\mathbf{L}_r$ contains six components which are the same for all v vertices run by index k.

The following manipulations of Eqs. (20) lead to a decoupled and easier-to-solve system:

(a) subtract the equation sets (20a) corresponding to a vertex, say m, from all the other equations (20a) to obtain

$$\boldsymbol{\varepsilon}_{kr}^{p^h} = \left(\mathbf{H}_{kr}^{h-1}\right)^{-1} \left\{ \lambda^h \left(\boldsymbol{\sigma}_{kr}^e - \boldsymbol{\sigma}_{mr}^e\right) + \mathbf{H}_{mr}^{h-1} \boldsymbol{\varepsilon}_{mr}^{p^h} \right\} \ , \tag{23}$$

(b) substitute Eq. (23) into Eq. (20d), so that the latter reads

$$\boldsymbol{\varepsilon}_{mr}^{p^h} = \left(\mathbf{H}_{mr}^{h-1}\right)^{-1} \left(\sum_{k=1}^{v} \left(\mathbf{H}_{kr}^{h-1}\right)^{-1} \right)^{-1} \left\{ \mathbf{B}_r \Delta\mathbf{U}^h + \lambda^h \sum_{k=1}^{v} \left(\mathbf{H}_{kr}^{h-1}\right)^{-1} \left(\boldsymbol{\sigma}_{mr}^e - \boldsymbol{\sigma}_{kr}^e\right) \right\}, \quad m = 1, \ldots, v \ ; \tag{24}$$

(c) substitute Eq. (24) into Eq. (20a) and, subsequently, this into Eq. (20b) to obtain

$$\left\{ \sum_{r=1}^{n} W_r |\mathbf{J}|_r \mathbf{B}_r^T \left(\sum_{k=1}^{v} \left(\mathbf{H}_{kr}^{h-1}\right)^{-1} \right)^{-1} \mathbf{B}_r \right\} \Delta\mathbf{U}^h = \lambda^h \sum_{r=1}^{n} W_r |\mathbf{J}|_r \mathbf{B}_r^T \left(\sum_{k=1}^{v} \left(\mathbf{H}_{kr}^{h-1}\right)^{-1} \right)^{-1} \sum_{k=1}^{v} \left(\mathbf{H}_{kr}^{h-1}\right)^{-1} \boldsymbol{\sigma}_{kr}^e \ ; \tag{25}$$

(d) substitute Eq. (24) into Eq. (20c) which thus becomes

$$\sum_{k=1}^{v} \sum_{r=1}^{n} W_r |\mathbf{J}|_r \boldsymbol{\sigma}_{kr}^{e^T} \left(\mathbf{H}_{kr}^{h-1}\right)^{-1} \left(\sum_{m=1}^{v} \left(\mathbf{H}_{mr}^{h-1}\right)^{-1} \right)^{-1} \times \left\{ \mathbf{B}_r \Delta\mathbf{U}^h + \lambda^h \sum_{m=1}^{v} \left(\mathbf{H}_{mr}^{h-1}\right)^{-1} \left(\boldsymbol{\sigma}_{kr}^e - \boldsymbol{\sigma}_{mr}^e\right) \right\} = 1 \ , \tag{26}$$

(e) denoting by $\mathbf{V}^h$ a new vector of N unknowns, substitute $\Delta\mathbf{U}^h = \lambda^h \mathbf{V}^h$ into Eq. (25), the solution of which numerically provides vector $\mathbf{V}^h$, say $\bar{\mathbf{V}}^h$,

(f) substitute now $\Delta\mathbf{U}^h = \lambda^h \bar{\mathbf{V}}^h$ into Eq. (26) to obtain the scalar λ^h, say $\bar{\lambda}^h$,

(g) finally, with $\bar{\lambda}^h$ and $\bar{\mathbf{V}}^h$ inserted in it as data, Eq. (24) provides the remaining unknowns $\boldsymbol{\varepsilon}_{mr}^{p^h}$ $(r = 1, \ldots, n,\ m = 1, \ldots, v)$.

The initialization of the iterative procedure (for $h = 1$) can be performed, like in [16, 25], by assuming that the whole solid is in a plastic state and, hence, by setting: $D_{kr}^0 = 1$ $(r = 1, \ldots, n,\ k = 1, \ldots, v)$.

Each iteration provides a value, say s^h, of the SD factor through Eq. (17a):

$$s^h = \sqrt{\tfrac{2}{3}} \sigma_0 \sum_{k=1}^{v} \sum_{r=1}^{n} W_r |\mathbf{J}|_r \sqrt{\boldsymbol{\varepsilon}_{kr}^{p^{T^h}} \mathbf{X} \boldsymbol{\varepsilon}_{kr}^{p^h}} \ . \tag{27}$$

The iterative procedure ends when a convergence criterion is satisfied, such as either $|s^{h-1} - s^h| / s^{h-1} \leq \delta_1$ or $\|\Delta\mathbf{U}^{h-1} - \Delta\mathbf{U}^h\| / \|\Delta\mathbf{U}^{h-1}\| \leq \delta_2$, where δ_1, δ_2 are suitable tolerances and $\|\ldots\|$ means Euclidean norm.

4.3 Remarks

The preceding kinematic formulation of the SD analysis and the above adopted solution algorithm give rise to the following reflections:

(i) The solution technique of Sec. 4.2 basically rests on the approach proposed in [26]. Noteworthy variants are: von Mises' material model which implies plastic incompressibility, instead of the ellipsoidal yield criterion, [26]; three-dimensional implementation for the SD analysis of technically meaningful structures, see Sec. 5.

(ii) The penalization adopted for the plastic incompressibility constraint exhibits some clear pros: "locking" phenomena are avoided because of the approximate "soft" enforcement of the constitutive kinematic constraints; no additional unknowns are involved. The main cons are: no general a-priori criterion is available for the choice of penalization parameter α, [3]; relatively small values α are expected to entail poor approximation of incompressibility; large values of α may imply numerical difficulties, in general, [27], and, specifically, may cause illconditioning of matrices $\mathbf{H}_{kr}$ to be inverted, see Eq. (21); in fact, it is easily seen on the basis of Eq. (21) that the condition number of $\mathbf{H}_{kr}$ increases linearly with α. The above trade-off can be only resolved on an empirical basis for each class of problems and, hence, motivates numerical investigations such as those in Sec. 5. Alternative anti-locking provisions can be found in literature, see e.g. [4].

(iii) Other user-available quantities, besides the convergence tolerances δ_1, δ_2, require problem-oriented numerical tests for suitable choices. These quantities are: parameters β for screening and splitting the Gauss point set G; parameter γ assumed to avoid singular coefficients.

(iv) The kinematic approach to SD leads to an assessment of the safety factor and a collapse mechanism defined by the resulting optimal vectors. The iteration sequence may be reduced by initializations of the adopted procedure based on conjectures concerning the collapse mechanism, frequently suggested by engineering judgement and/or by previous numerical experience.

5
Applications and comparisons

5.1
Validation by two-dimensional analyses

First, some SD analyses available in the literature are used below for comparisons with the present method. For the case with geometry, finite element mesh and loading domains ($v = 4$ vertices) illustrated in Fig. 1, the main assumptions are: plane-stress states; von Mises' elastic-plastic material model; displacement modelling by 200 four-node isoparametric finite elements; chosen available parameters $\beta = \gamma = 10^{-10}$, Eq. (22), for screening Gauss points and defining yielding and nonyielding zones; convergence tolerances $\delta_1 = \delta_2 = 10^{-5}$. The plane stress hypothesis makes the plastic incompressibility constraint implicit and, therefore, penalization and the relevant factor α do not apply.

Some results of numerical tests based on the above data are illustrated in Fig. 2. The SD domain in Fig. 2a is the envelope of all load domains in Fig. 1c for varying $p_1^{\max}$ and $p_2^{\max}$ ($0 \le p_1 \le p_1^{\max},\ 0 \le p_2 \le p_2^{\max}$), amplified to the computed SD limits. Reasonable agreement is observed in Fig. 2a with the counterpart result in [6], achieved by piecewise linearization of the yield criterion and linear programming starting from the same data. Some numerically detailed comparisons with earlier works are as follows: for $p_1^{\max} = p_2^{\max}$ (for $p_2^{\max} = 0$ the results are in

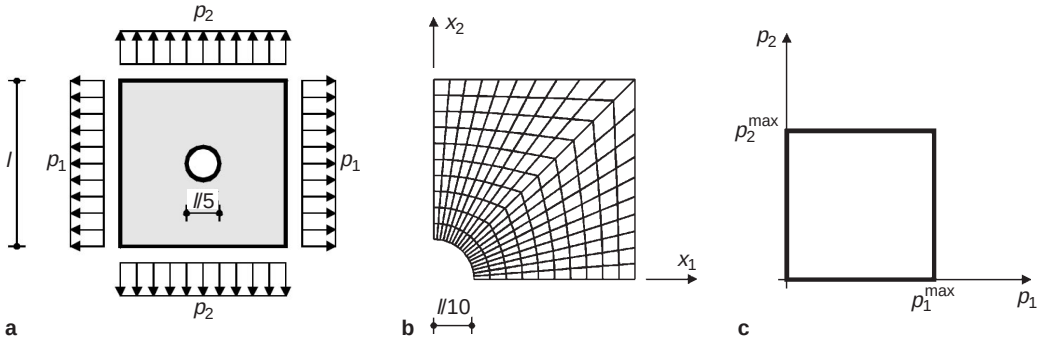

Fig. 1. Thin plate with a central hole: (a) geometry; (b) finite element mesh; (c) loading domain

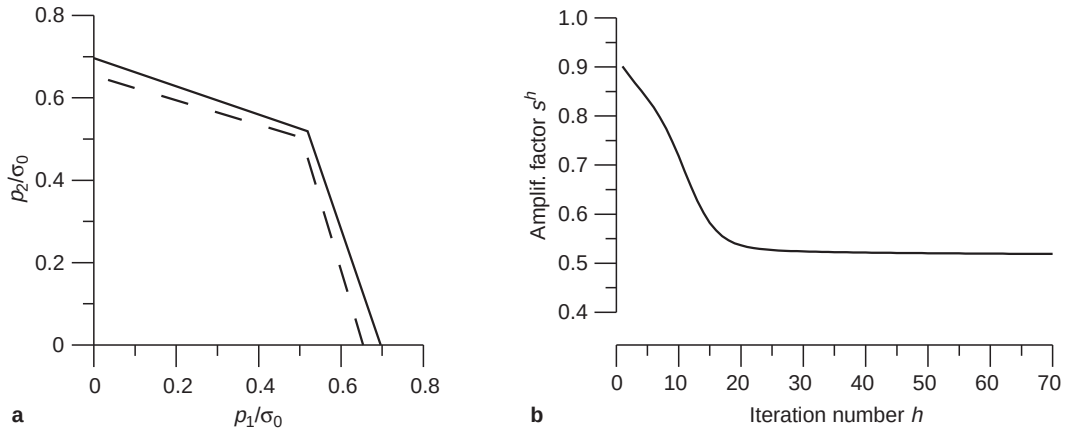

Fig. 2. **a** Shakedown domain for the problem of Fig. 1: solid line by present method, dashed line from [6]; **b** convergence for $p_1^{\max} = p_2^{\max}$

parentheses) we get $s = 0.518$ (0.696) by the present method; $s = 0.502$ (0.654) in [6]; $s = 0.431$ in [2] by a static approach; $s = 0.556$ in [1] by a kinematic approach; $s = 0.478$ (0.653) in [7].

Figure 2b shows a typical behaviour of the load factor sequence s^h as a function of the iteration number h and its convergence on the sought SD limit for $\gamma = 10^{-10}$. In this case, γ is the only available parameter; other numerical tests have been performed for $\gamma = 10^{-6}/10^{-12}$ with negligible consequences both on the optimal value s and the convergence speed. Whereas $\gamma = 10^{-16}$ gives rise to numerical troubles which materialize in early interruption of the iteration sequence.

5.2
Damaged pipelines with fluctuating pressure

In certain circumstances, pressure vessels and pressurized pipelines are exposed to damages (caused, e.g. by pitting corrosion), which materialize in part-through cavities or slots. The idealized geometry of the considered defective cylinders and the relevant parameters are defined in Fig. 3.

For the present computational tests, like for limit analysis in [16], the following geometric data (in mm) have been adopted with reference to Fig. 3: $R_e = 120$, $R_i = 100$, $t = 20$; $b = 13$; spherical slot: $L = 300$, $c = 20$, $w = 20$; circumferential ellipsoidal slot: $L = 300$, $c = 10$, $w = 30$; axial ellipsoidal slot: $L = 300$, $c = 60$, $w = 20$; rectangular ellipsoidal slot: $L = 420$, $c = 140$, $w = 20$.

The material model assumed is the usual von Mises' elasto-plasticity, now with the parameters $E = 2.1 \times 10^5$ MPa; $\nu = 0.3$; $\boldsymbol{\sigma}_0 = 200$ MPa.

The external actions consist of internal pressure p, fluctuating between 0 and $p^{\max}$, and of axial tensile traction uniformly acting on plane $x_3 = L$ with resultant equal to $\pi R_i^2 p$ (load domain with $v = 2$ vertices, one of which is the unloaded situation). The assumed symmetries, including one with respect to the axial horizontal plane $x_2 = 0$, are exploited as shown in Fig. 3.

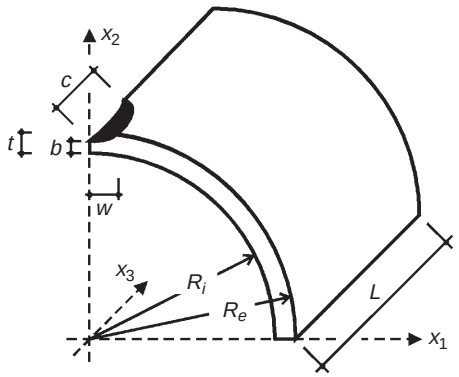

Fig. 3. Pressure vessels with part-through slots: geometric parameters

The space discretization is performed by isoparametric eight-node finite elements with eight Gauss points, their number is varying between 600 and 850, depending on the slot geometry; a typical mesh is depicted in Fig. 4.

The following results of the parametric analyses carried out in this study are worth to be pointed out.

For the various slot geometries considered, Table 1 exhibits the collapse pressures provided by: (1) the present method (first column); (2) the commercial code ABAQUS (second one); (3) the present method, specialized to limit analysis (third), [16]; (4) the code ABAQUS, assuming monotonic increasing pressure like for the limit analysis (fourth column).

Evolutive time-marching analyses performed by a nonlinear commercial code (such as ABAQUS), if used to establish the SD limit s, provide an abundant amount of irrelevant information. They must be carried out over a number of loading cycles, and repeated by trial-and-error for increasing peak pressures, by monitoring the cumulative dissipated energy, as shown in Fig. 5, in order to capture the threshold between bounded and unbounded cumulative dissipation. Clearly, such computational exercises turn out to be expensive. Typically quantified by the following representative computing CPU times (in sec., on a HP workstation) they emerge from the present study as follows: for the spherical slot 120000 vs. 500; for rectangular ellipsoidal slot 170000 vs. 500, (the former figures concern the evolutive analyses by ABAQUS, the latter the direct SD analyses).

Figure 4 shows, for the axial ellipsoidal slot geometry, the incremental collapse mechanisms provided by direct kinematic SD analysis, Fig. 4a, and by the time-marching analysis, Fig. 4b. In the former method, this mechanism is defined straightforwardly by the optimal vector of the minimization problem; in the latter analysis the same information can be derived approximately from the increments of residual displacements over some loading cycles.

In Fig. 6, the plastic collapse pressure is compared to the incremental collapse pressure, both made dimensionless by relating to the limit pressure of the undamaged vessel, as functions of longitudinal length c of the slot, having set $w = 20$ mm and R_i, R_e, b, t, L equal to the above-assumed values. It is worth noting that inadaptation by incremental collapse occurs for

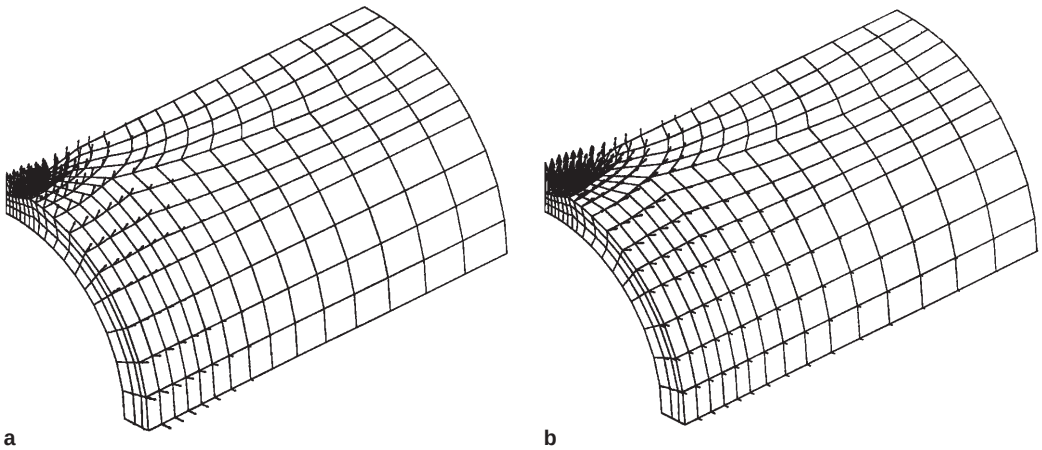

Fig. 4a, b. Pressure vessel with axial ellipsoidal slot. Incremental collapse mechanism from **a** present method; **b** ABAQUS

Table 1. Collapse pressures (in MPa) resulting from the shakedown analysis (SD) and limit analysis (LA), by direct and evolutive approaches

	SD Present method	SD ABAQUS	LA [16]	LA ABAQUS
Without slot	42.2	42.1	42.2	42.1
Spherical slot	40.42	40.1	40.55	40.7
Circumf. ellipsoidal slot	41.11	41.2	41.25	41.7
Axial ellipsoidal slot	35.50	36.0	38.97	40.1
Rectangular slot	29.95	32.7	33.96	34.4

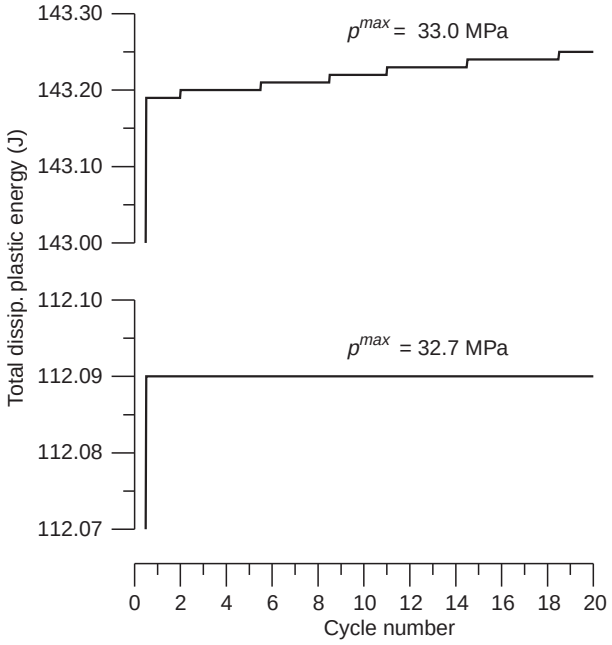

Fig. 5. Evolutive SD analysis of a vessel with rectangular part-through slot: cumulative dissipation versus cycle number for two values of the peak pressure $p^{\max}$

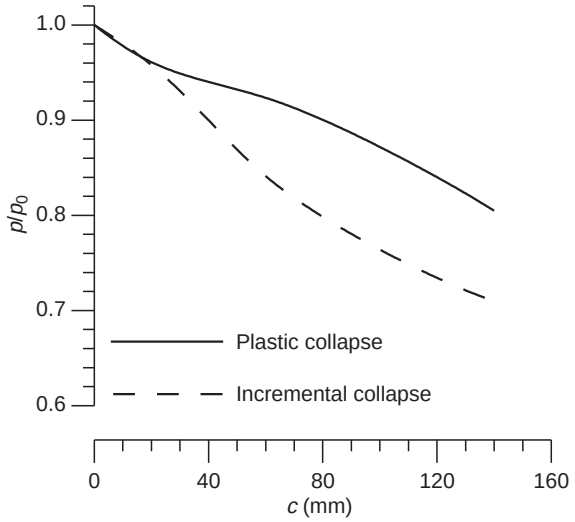

Fig. 6. Plastic collapse and incremental collapse pressures (p_0 denotes the limit pressure of the undamaged vessel) versus the longitudinal length of the slot c, for w = 20 mm

pressure peaks substantially lower than plastic collapse pressures except for small lengths c (say, below the thickness). This notable circumstance corroborates the need for the SD analysis in practical assessment of the integrity of pressurized vessels.

In the present 3D situations, the penalization factor α for the enforcement of plastic incompressibility is, naturally, expected to play an important role in the numerical solution of the SD analysis. Its role has been investigated, and results concerning the vessel with axially ellipsoidal slot are plotted in Fig. 7, having set $\gamma = 10^{-8}$ and $\delta_1 = \delta_2 = 10^{-3}$. The interval from $\alpha = 10^2$ to $\alpha = 10^{18}$ has been scanned: $\alpha = 10^3$ and lesser values lead to erroneous SD limits, significantly lower than the actual one ($p \approx 35.5$ MPa); on the other end, $\alpha > 10^{16}$ gives rise to higher erroneous SD limits, fast increasing with α. Clearly, the former circumstance, i.e. a weak penalization, reflects an excessive relaxation of the kinematic constraints in the system; the latter fact is a locking manifestation due to excessively stiff penalization. The practically remarkable result is the large amplitude of the α interval leading to correct SD limit. Unfortunately, this conclusion cannot be generalized, but turns out to be problem-dependent. In fact, a similar investigation carried out in the study for 2D plane-strain problems led to a narrower interval of admissible penalization factors α.

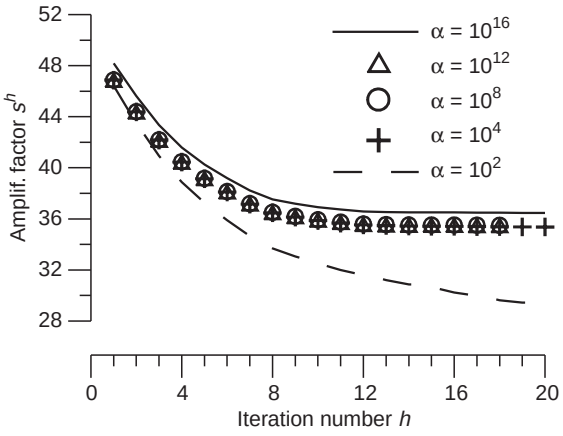

Fig. 7. Convergence of the amplification factor in the direct SD analyses of a vessel with axial ellipsoidal slot ($\gamma = 10^{-8}$)

The assumed horizontal symmetry (Fig. 4) is warranted by the localized geometry of the slots and by the expected empirical fact that its removal negligibly alters the limit and SD analysis results. The removal of that symmetry has implied a meaningful numerical test: the consequent increase in the number of variables entailed an almost proportional growth of computing time for the present numerical procedure. Specifically, for rectangular slots as a representative example: nodal d.o.f. from 3024 (756 FEs) to 4536 (1134 FEs); limit analysis from 400 to 970 CPU sec.; SD analysis from 560 to 1200 CPU sec. However, clearly, the above encouraging remark cannot be generalized to problem size growth by mesh refinements.

6
Conclusions

The study expounded in this paper leads to the following conclusions:

(a) Shakedown (SD) finite element analysis by the kinematic approach can be efficiently performed with the enforcement of the plastic incompressibility by penalization, by solving the (nonlinear) stationarity conditions of the Lagrangian function, using a suitably adjusted iterative procedure proposed in [16, 25]. This procedure turns out to be significantly cost-effective with respect to other approaches, particularly with respect to evolutive step-by-step analyses by commercial finite element codes. This conclusion has been corroborated by means of a three-dimensional implementation carried out in this study and by numerical tests concerning practical engineering situations, such as defective pressure vessels.

(b) The numerical behaviour (in particular, its convergence speed) of the solution procedure adopted herein appears to be satisfactory and rather insensitive to the choice of the initialization vector and of the user-available parameters (penalization factor α; parameters β and γ screening rigid-yielding zones). However, the optimal choice of these parameters is dependent on essential geometrical features of the kind of problems considered and rests merely on empirical bases.

(c) Penalization turns out to be a convenient and effective way of achieving a practically satisfactory compromise between the conflicting requirement of enforcing plastic incompressibility and avoiding "locking" in finite element analyses.

(d) The specialization of the present SD analysis technique to the limit analysis has made evident a significant conservativeness of some semi-empirical formulae currently employed in industrial environments, [22].

(e) Extensions to elasto-plastic material models more general than von Mises' perfect elasto-plasticity adopted here, would preserve the nonsmoothness of the objective function, but it would imply diverse mathematical features (such as nonconvex equality constraints for Drucker-Prager model, instead of convex like for von Mises, see e.g. [5]) which appear to be worth studying as for the performance of the kind of iterative algorithm investigated here.

(f) Although the application is focused here on 3D structures (defective pressure vessels), the present kinematic formulation is general and can be implemented with any type of kinematically admissible finite element (e.g. pipe element, shell element, 2D or 3D solid element, etc.). In particular, the present method can be applied to shell and pipe structures of nuclear, oil and other industries. The loading domain can be considered to include more complex loading such as combinations of variable repeated thermal and mechanical external actions, also in the presence of dead loads.

References

1. **Aboustit, B.; Reddy, D. V.:** Finite element linear programming approach to foundation shakedown. Proc. Int. Symposium on Soil under Cyclic and Thermal Loading, Swansea, 7–11 January 1980
2. **Belytschko, T.:** Plane stress shakedown analysis by finite elements. Int. J. Mech. Sci. 14 (1972) 619–625
3. **Bertsekas, D. P.:** Constrained Optimization and Lagrange Multiplier Methods. Boston: Academic Press Inc. 1982
4. **Capsoni, A.; Corradi, L.:** A finite element formulation of the rigid-plastic limit analysis problem. Int. J. Numer. Methods Eng. 40 (1997) 2063–2086
5. **Corigliano, A.; Maier, G.; Pycko, S.:** Dynamic shakedown analysis and bounds for elastoplastic structures with nonassociative, internal variable constitutive laws. Int. J. Solids and Structures, 32 (1995) 3145–3166
6. **Corradi, L.; Zavelani, A.:** A linear programming approach to shakedown analysis of structures. Comput. Methods Appl. Mech. Eng. 3 (1974) 37–53
7. **Genna, F.:** A nonlinear inequality, finite element approach to the direct computation of shakedown load safety factors. Int. J. Mech. Sci. 30 (1988) 769–789
8. **Kaliszky, S.:** Plasticity. Theory and Engineering Applications. Amsterdam: Elsevier 1989
9. **Kamenjarzh, J.; Merzljakov, A.:** On kinematic method in shakedown theory: I. Duality of extremum problems. Int. J. Plasticity 10 (1994) 363–380
10. **Kamenjarzh, J.; Merzljakov, A.:** On kinematic method in shakedown theory: II. Modified kinematic method. Int. J. Plasticity 10 (1994) 381–392
11. **Karadeniz, S.; Ponter, A. R. S.:** A linear programming upper bound approach to the shakedown limit of thin shells subjected to variable thermal loading. J. Strain Anal. 19 (1984) 221–230
12. **Koiter, W. T.:** A new general theorem on shake-down of elastic-plastic structures. Proc. Kon. Ned. Akad. Wet. B59 (1956) 24–34
13. **König, J. A.; Kleiber, M.:** On a new method of shakedown analysis. Bulletin de l'Académie Polonaise des Sciences – Série des sciences techniques 26 (1978) 165–171
14. **König, J. A.; Maier, G.:** Shakedown analysis of elastoplastic structures: a review of recent developments. Nucl. Eng. Des. 66 (1981) 81–95
15. **König, J. A.:** Shakedown of Elastic-Plastic Structures. Amsterdam: Elsevier 1987
16. **Liu, Y. H.; Cen, Z. Z.; Xu, B. Y.:** A numerical method for plastic limit analysis of 3-D structures. Int. J. Solids Struct. 32 (1995) 1645–1658
17. **Liu, Y. H.; Cen, Z. Z.; Xu, B. Y.:** Numerical limit analysis of cylindrical shells with part-through slots. Int. J. Pres. Ves. & Piping 64 (1995) 73–82
18. **Lubliner, J.:** Plasticity theory. New York: Macmillan Publishing Company 1990
19. **Maier, G.:** Shakedown theory in perfect elastoplasticity with associated and nonassociated flow-laws: a finite element, linear programming approach. Meccanica 4 (1969) 250–260
20. **Maier, G.:** A shakedown matrix theory allowing for workhardening and second-order geometric effects. In: Sawczuk (ed.), Inter. Sympos. on Foundations of Plasticity. Warsaw 1972
21. **Melan, E.:** Zur Plastizität des räumlichen Kontinuums. Ing. Archiv 8 (1938) 116–126
22. **Miller, A. G.:** Review of limit loads of structures containing defects, Int. J. Pres. Ves. & Piping 32 (1988) 197–327
23. **Morelle, P.:** Numerical shakedown analysis of axisymmetric sandwich shells: an upper bound formulation. Int. J. Numer Methods Eng. 23 (1986) 2071–2088
24. **Symonds, P. S.; Neal, B. G.:** Recent progress in the plastic method of structural analysis. Part I. J. Franklin Inst. 252 (1951) 383–407
25. **Zhang, Y. G.; Zhang, P.; Lu, M. W.:** Computational limit analysis of rigid-plastic bodies in plane strain. Acta Mech. Solida Sinica 6 (1993) 341–348
26. **Zhang, Y. G.:** An iterative algorithm for kinematic shakedown analysis. Comput. Methods Appl. Mech. Eng. 127 (1995) 217–226
27. **Zienkiewicz, O. C.; Taylor, R. L.:** The Finite Element Method. London: McGraw-Hill 1994